Supporting Information

Ultrasensitive Cracking-assisted Strain Sensors Based on Silver Nanowires/Graphene Hybrid Particles

Song Chen, Yong Wei, Siman Wei, Yong Lin, Lan Liu*

College of Materials Science and Engineering, Key Lab of Guangdong Province for High Property and Functional Macromolecular Materials, South China University of Technology, Guangzhou 510640, P. R. China.

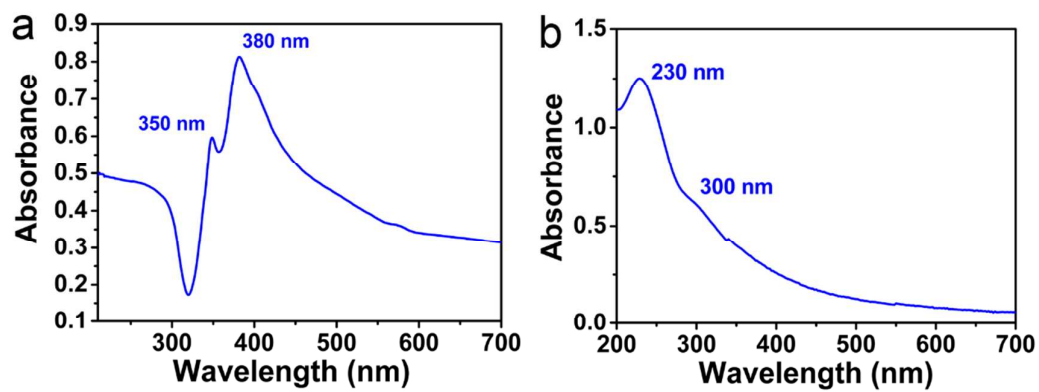** Corresponding to Lan Liu   E-mail: psliulan@scut.edu.cn*

Figure S1. Ultraviolet–visible spectra of AgNWs solution (a) and GO solution (b) with concentration of 0.05 mg ml^{-1}
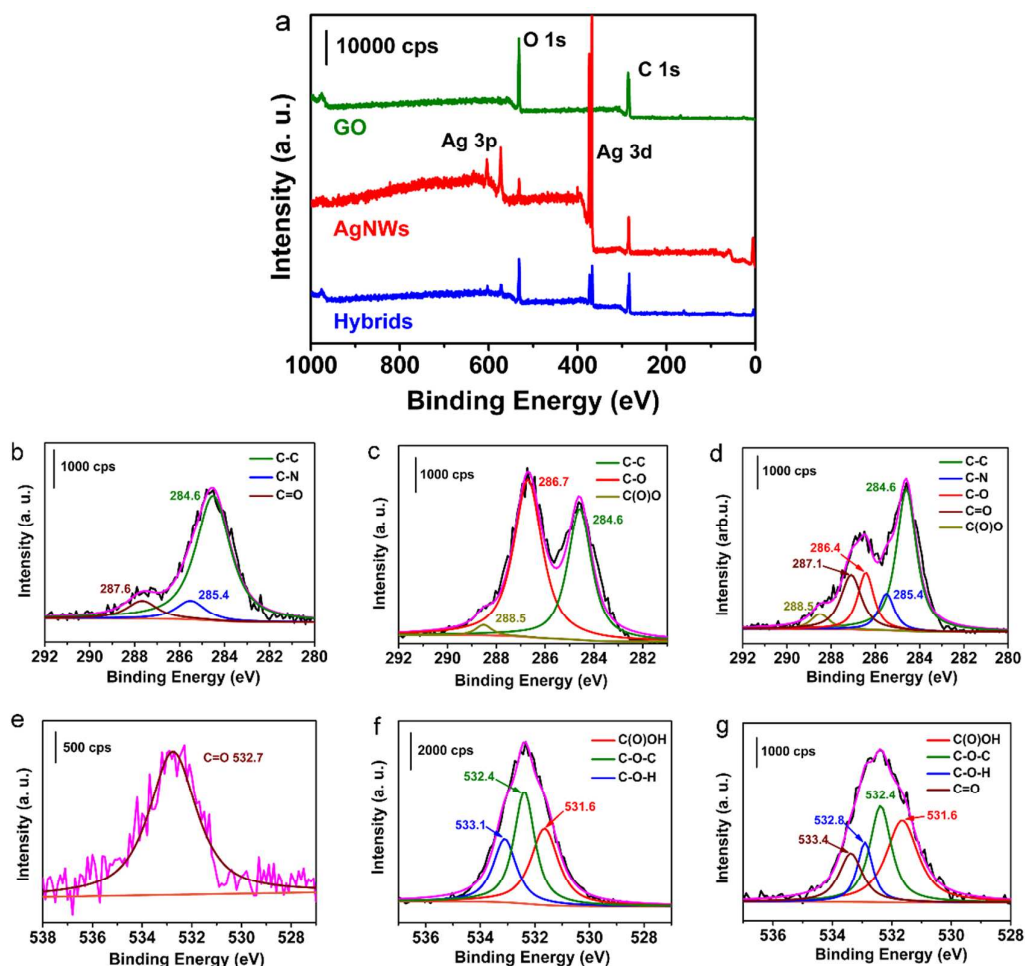
Figure S2. (a) XPS wide-scan spectrums of AgNWs, GO and their coprecipitation; high resolution XPS spectrums of C1s for AgNWs (b), graphene oxides (c) and their coprecipitation (d); high resolution XPS spectrums of O1s for AgNWs (e), graphene oxides (f) and their coprecipitation (g).

As illustrated in Figure S2 (a), all the spectrums are referenced to C 1s peak (binding energy = 284.6 eV).[1] High-resolution spectra of C 1s are shown in Figure S2b, c and d, the C 1s region in Figure S2b for original AgNWs can be fitted into three peaks at 284.6 eV, 285.4 eV, 287.6 eV corresponding to C-C, C-N and C=O, respectively, this is due to the absorption of PVP on the surface of AgNWs. The C 1s for original GO can also be fitted into three peaks at 284.6 eV, 286.7 eV, 288.5 eV as shown in Figure S2c ascribed in C-C, C-OH and C(O)O, respectively. After coprecipitation, the peaks assigned to C=O for AgNWs and C-O for GO shift to 287.1

eV and 286.4 eV because of the charge transfer from AgNWs to GO (see Figure S2d). The XPS spectra of O 1s were also investigated. The O 1s region in Figure S2e for AgNWs shows there only one peak at 532.7 eV attributed to C=O group of PVP, The O 1s high-resolution spectra for GO can be fitted into three peaks at 531.6 eV, 532.4 eV, 533.1 eV as shown in Figure S2f assigned to C(O)OH, C-O-C and C-O-H, respectively. Similar to the C 1s spectrums, the peaks assigned to C=O for AgNWs and C-O-H for GO shift to 533.4 eV and 532.8 eV after coprecipitation (Figure S2g). Since there are about 2 nm PVP on the surface of AgNWs and a large number of hydroxyl groups on GO nanosheets, hydrogen bonding can be formed between AgNWs and GO. It is the reason for easily assembly of AgNWs and GO nanosheets.
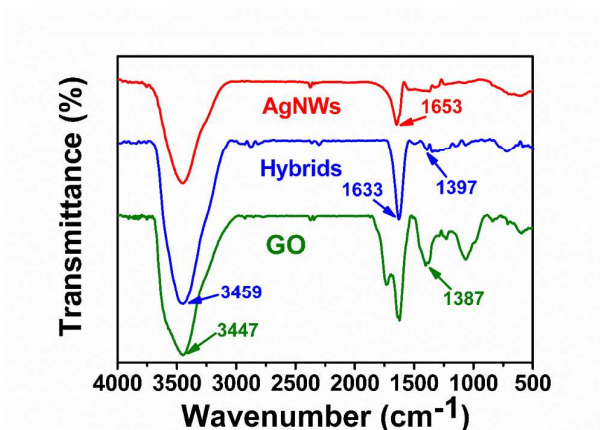

Figure S3. FTIR spectrums for AgNWs, GO and their hybrids.

As shown in Figure S3, for AgNWs, the peaks at 1653 cm^{-1} belongs to the stretching vibration of C=O groups on the PVP molecular chain. And for GO, the characteristic peaks of –OH groups appear at 3447 cm^{-1} and 1387cm^{-1}, corresponding to the vibration and deformation peaks of -OH groups.[2] After coprecipitation, the

FTIR spectrum of hybrids is also measured in Figure S3. For hybrids, the peaks for C=O groups shift from 1653 cm^{-1} to 1633 cm^{-1}. This is because that the hydrogen bonding interaction between C=O groups and –OH groups cause the electronic cloud density of C=O groups to decrease. Similarly, for hybrids, the vibration and deformation peaks for –OH groups shift to 3459 cm^{-1} and 1397cm^{-1}, respectively. It can also confirm the hydrogen bonding interaction between AgNWs and GO nanosheets.
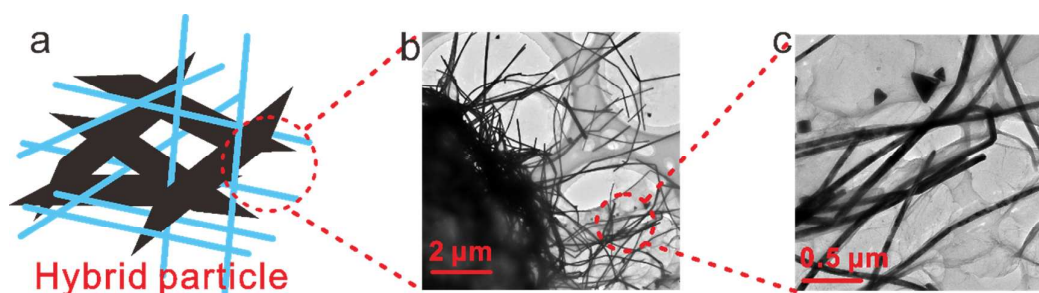

Figure S4. (a) Schematic illustration of a hybrid particle. (b, c) TEM image of hybrid particle (b) and the closeup image of the particle edge (c).
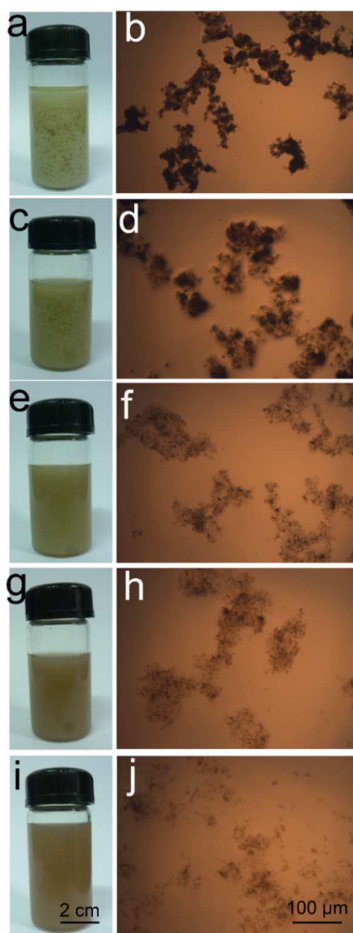
Figure S5. Digital photographers of as-prepared hybrid particles and their corresponding optical microscope images with AgNWs and GO proportion of 4:1 (a, b), 2:1 (c, d), 1:1 (e, f), 1:2 (g, h), 1:4 (i, j)
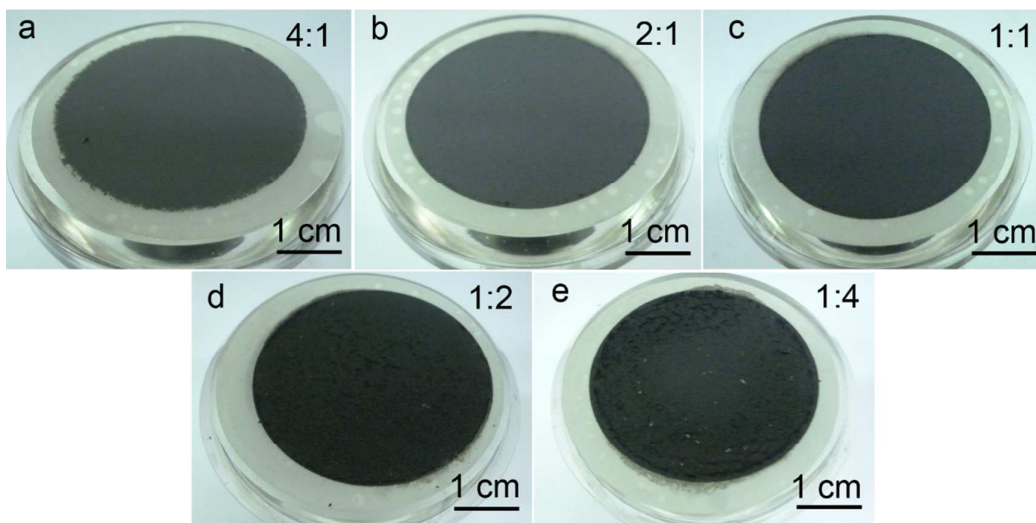
Figure S6. Digital photographers of as-prepared hybrid membranes with AgNWs and GO proportion of 4:1 (a), 2:1 (b), 1:1 (c), 1:2 (d), 1:4 (e)
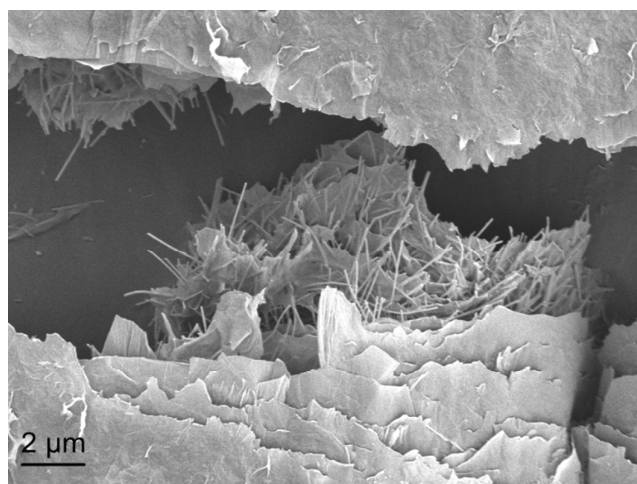

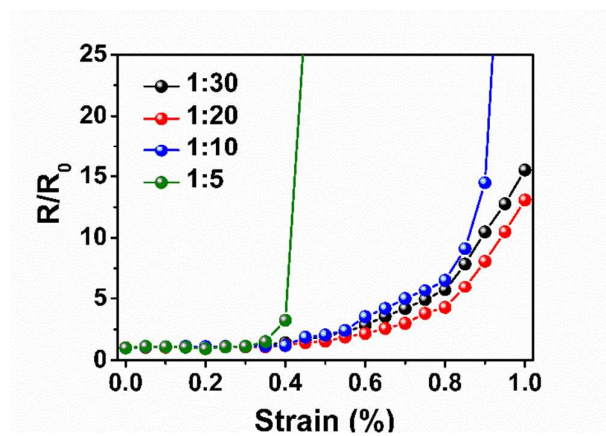Figure S7. SEM image of strain sensor under 50% strain shows the micro morphologies of SGHPs

Figure S8. Change in resistance as a function of strain with different layer thickness

proportions.

Table S1: The comparison of gauge factor under 1% strain between recently reported strain sensors and our work

References	Materials	Gauge factor($\Delta\varepsilon \leq 1\%$)
3	Vertically aligned and sparse SWCNT thin films	0.82
4	Multi-wall carbon nanotube entangled networks	4
5	Gold nanoparticles	100
6	Graphene woven fabrics	800
7	Carbon and functionalized carbon nanotubes	5
8	Multi-wall carbon nanotube	5.39
9	Cracks-based Pt film	800
10	Graphene with "Compression spring" structure	10
11	Gold films	96
12	carbonized polyimide	50
13	Gold nanoparticle	300
14	Microfluidic	2
15	Graphene on hair	4.47
16	Graphite draw by pencil	536.61
17	Thickness-gradient films of CNTs	100
18	Channel cracks-based gold	5000
19	ZnO piezoelectric fine-wires	1200
20	Cracks-based graphite	26.9
21	Graphite	804.9
This work	Graphene and Ag nanowires hybrid particles	4000

Reference:

[1] Li, J.; Tang, S.; Lu, L.; Zeng, H. C. Preparation of Nanocomposites of Metals, Metal Oxides, and Carbon Nanotubes via Self-Assembly. *J. Am. Chem. Soc.* **2007**, 129, 9401–9409

[2] Ma, Q.; Song, J.; Jin, C.; Li, Z.; Liu, J.; Meng, S., Zhao, J.; Guo, Y. A Rapid and Easy Approach for the Reduction of Graphene Oxide by Formamidinesulfinic Acid. *Carbon* **2013**, 54, 36 – 41

[3] Yamada, T.; Hayamizu, Y.; Yamamoto, Y.; Yomogida, Y.; Izadinajafabadi, A.;

Futaba, D. N.; Hata, K.; A Stretchable Carbon Nanotube Strain Sensor for Human-Motion Detection. *Nat. Nanotechnol.* **2011**, 6, 296-301

[4] Slobodian, P.; Riha, P.; Saha, P. A Highly-Deformable Composite Composed of An eEntangled Network of Electrically-Conductive Carbon-Nanotubes Embedded in Elastic Polyurethane. *Carbon* **2012**, 50, 3446-3453.

[5] Farcau, C.; Sangeetha, N. M.; Moreira, H.; Viallet, B.; Grisolia, J.; Ciuculescupradines, D.; Ressier, L. High-Sensitivity Strain Gauge Based on a Single Wire of Gold Nanoparticles Fabricated by Stop-and-Go Convective Self-Assembly. *ACS Nano* **2011**, 5, 7137-43.

[6] Li, X.; Zhang, R.; Yu, W.; Wang, K.; Wei, J.; Wu, D.; Cao, A.; Li, Z,; Cheng, Y.; Zheng, Q.; Ruoff, R. S.; Zhu, H. Stretchable and Highly Sensitive Graphene-on-Polymer Strain Sensors. *Sci. Rep.* **2012**, 2, 870.

[7] Lin, L.; Liu, S.; Qi, Z.; Li, X.; Ji, M.; Hua, D.; Fu, Q. Towards Tunable Sensitivity of Electrical Property to Strain for Conductive Polymer Composites Based on Thermoplastic Elastomer. *ACS Appl. Mater. Interfaces* **2013**, 5, 5815-5824.

[8] Duan, L.; Fu, S.; Deng, H.; Zhang, Q.; Wang, K.; Chen, F.; Fu, Q.; The Resistivity–Strain Behavior of Conductive Polymer Composites: Stability and Sensitivity. *J. Mater. Chem. A* **2014**, 2, 17085–17098

[9] Kang, D.; Pikhitsa, P. V.; Choi, Y. W.; Lee, C.; Shin, S. S.; Piao, L.; Park, B.; Suh, K. Y.; Kim, T.; Choi, M. Ultrasensitive Mechanical Crack-based Sensor Inspired by The Spider Sensory System. *Nature* **2014**, 516, 222-226

[10] Cheng, Y.; Wang, R.; Sun, J.; Gao, L. A Stretchable and Highly Sensitive Graphene-Based Fiber for Sensing Tensile Strain, Bending, and Torsion. *Adv. Mater.* **2015**, 27, 7365–7371

[11] Filiatrault, H. L.; Carmichael, R. S.; Boutette, R. A.; Carmichael, T. B. A Self-Assembled, Low-Cost, Microstructured Layer for Extremely Stretchable Gold Films, *ACS Appl. Mater. Interfaces* **2015**, 7, 20745−20752

[12] Rahimi, R.; Ochoa, M.; Yu, W.; Ziaie, B. Highly Stretchable and Sensitive Unidirectional Strain Sensor via Laser Carbonization. *ACS Appl. Mater. Interfaces* **2015**, 7, 4463−4470

[13] Yi, L.; Jiao, W.; Wu, K.; Qian, L.; Yu, X.; Xia, Q.; Mao, K.; Yuan, S.; Wang, S.; Jiang, Y. Nanoparticle Monolayer-Based Flexible Strain Gauge with Ultrafast

Dynamic Response for Acoustic Vibration Detection. *Nano Res.* **2015**, 8, 2978-2987.

[14] Yoon, S. G.; Koo, H. J.; Chang, S. T. Highly Stretchable and Transparent Microfluidic Strain Sensors for Monitoring Human Body Motions. *ACS Appl. Mater. Interfaces* **2015**, 7, 27562−27570

[15] Yuan, W.; Zhou, Q.; Li, Y.; Shi, G. Small and Light Strain Sensors Based on Graphene Coated Human Hairs. *Nanoscale* **2015**, 7, 16361-16365.

[16] Liao, X.; Liao, Q.; Yan, X.; Liang, Q.; Si, H.; Li, M.; Wu H.; Cao S.; Zhang Y. Flexible and Highly Sensitive Strain Sensors Fabricated by Pencil Drawn for Wearable Monitor, *Adv. Funct. Mater.*, **2015**, 25, 2395–2401

[17] Liu, Z.; Qi, D.; Guo, P.; Liu, Y.; Zhu, B.; Yang, H.; Liu, Y.; Li, B.; Zhang, C.; Yu, J.; Liedberg, B.; Chen, X. Thickness-Gradient Films for High Gauge Factor Stretchable Strain Sensors. *Adv. Mater.* **2015**, 27, 6230–6237

[18] Yang, T.; Li, X.; Jiang, X.; Lin, S.; Lao, J.; Shi, J.; Zhen, Z.; Li, Z.; Zhu, H. Structural Engineering of Gold Thin Films with Channel Cracks for Ultrasensitive Strain Sensing. *Mater. Horiz.* **2016**, 3, 248-255

[19] Zhou, J.; Gu, Y.; Fei, P.; Mai, W.; Gao, Y.; Yang, R.; Bao, G.; Wang, Z. L. Flexible piezotronic strain sensor. *Nano Lett.* **2008**, 8, 3035-3040.

[20] Amjadi, M.; Turan, M.; Clementson, C. P.; Sitti, M. Parallel Microcracks-based Ultrasensitive and Highly Stretchable Strain Sensors. *ACS Appl. Mater. Interfaces* **2016**, 8, 5618−5626

[21] Liao, X.; Zhang, Z.; Liao, Q.; Liang, Q.; Ou, Y.; Xu, M.; Li, M.; Zhang, G.; Zhan, Y. Flexible and Printable Paper-based Strain Sensors for Wearable and Large-area Green Electronics. *Nanoscale* **2016**, 8, 13025-13032